

## **Petrophysical Evaluation and Reservoir Modeling of Oligocene succession in Bai-Hassan oil field, Northern Iraq**

**<sup>1</sup>Dalya K\*, <sup>2</sup>Fawzi M. Al-Beyati, and <sup>3</sup>Mazin Y. Tamar-Agha**

---

### **Author's Affiliations:**

<sup>1</sup>Department of Petroleum Engineering, College of Engineering, Al-Kitab University, Iraq

<sup>2</sup>Engineering Technical College of Kirkuk, Northern Technical University, Iraq

<sup>3</sup>Department of Geology, College of Sciences, University of Baghdad, Iraq

**\*Corresponding Author: Dalya K,** Department of Petroleum Engineering, College of Engineering, Al-Kitab University, Iraq

**E-mail:** dalia.kamran9@gmail.com

(Received on 25.11.2022, Revised on 25.01.2023, Approved on 28.01.2023, Accepted on 08.02.2023, Published on 15.06.2023)

---

**How to cite this article:** Dalya K., Fawzi M. Al-Beyati, and Mazin Y. Tamar-Agha (2023). Petrophysical Evaluation and Reservoir Modeling of Oligocene succession in Bai-Hassan oil field, Northern Iraq. *Bulletin of Pure and Applied Sciences- Geology*, 42F(1), 64-87.

---

### **Abstract:**

Bai-Hassan Oil Field is considered as one of the important north Iraq oil fields. The oil field of Bai-Hassan is faraway about 40 km to the northwest of Kirkuk City. The field consists of two domes (in NW- SE direction) Kithka Dome and Dauod Dome separated by a narrow saddle called Shashal saddle. The current study is focused on microfacies analysis to build 3D reservoir models and petrophysical properties of Palani Formation (Early Oligocene) and Baba, Bajawan and Tarjil formations (Middle Oligocene). In the present study, several types of well-logs obtained from BH-20, BH-39, BH-53, BH-89, BH-91, BH-92, and BH-122 wells which including gamma-ray (GR), neutron (NPHI), density (ROHB), sonic (DT), spontaneous potential (SP) and resistivity (LLD, MSFL) well-logs were used in order to determine and study of reservoir characterization to explain different parameters including lithology with contacts identifications, total (PHIT) and effective (PHIE) porosities, permeability, water saturation (SW) and hydrocarbons saturation (Sh), of Oligocene succession in the Bai-Hassan Oil Field within Zagros basin, northern Iraq. The analysis of the results showed that the Kathka dome area compared to the Dauod dome area is better in terms of petrophysical properties as well as in terms of its content of hydrocarbon groups.

**Keywords:** Petrophysical Evaluation; Reservoir Modeling; Oligocene succession; Bai-Hassan oil field; Northern Iraq

---

### **1. INTRODUCTION**

Petroleum reservoir is a bed of rock that could hold gas, oil, and water. A commercially productive reservoir must have sufficient thicknesses and pores-space to include a large hydrocarbons values and must yield fluids at the

rate satisfactory when the reservoirs are penetrating (Brock, 1986).

Well-logs have been used to calculate of the essential parameters like porosity and permeability (Albeyati et al.,2021), in addition to the calculation the amount of both oil and gas in

the field. It's a graph that shows the depth of a well versus a rock property or characteristic. Carottage électrique, literally "electrical coring," is the French version of the word "well logging," which would have been a reasonably accurate definition of this geophysical oil and gas exploration approach when it was invented in 1927 (Hingle, 1959 and Pickett, 1968).

Well-logs have been used to calculate petrophysical parameters and the amount of oil and gas in the studied field. Well-logs can't and predict porosity or hydrocarbon saturation directly. The calculation parameters of porosity and saturation either water and oil, equations were prepared according to mathematical or empirical models of the rocks behavior (Etne, 1990).

Reservoir assessment aims to identify the spatial carbonates distribution characteristics, sandstone, and shales reservoir units both qualitative and quantitative as well as simulation the production and storage status of hydrocarbons in these rocks. However, reservoir evaluation can be determined using a variety of parameters including well logging data, petrography, microfacies, and cores analysis study. The well-logging petrophysics parameter is the most important and useful available tools to petroleum geologists (Asquith and Krygowski, 2004).

Several parameters and properties of the rock units can be observed from the interpretation of well logging such as petrography, microfacies, and core analytical studies. However, petrophysical well logging interpretation represents the most significant and valuable techniques applied for petroleum geology (Asquith and Krygowski, 2004).

In the current study, several types of well-logs obtained from BH-20, BH-39, BH-53, BH-89, BH-91, BH-92, and BH-122 boreholes are gamma ray, neutron, density, acoustic (DT) and resistivity (LLD, MSFL) well-logs were used in order to determine and study of reservoir characterization to explain different parameters including total and effective porosities, permeability, water saturation (SW) and hydrocarbons saturation (Sh), of Oligocene succession in the Bai-Hassan oilfield from northern Iraq.

Bai-Hassan giant oil field is sited within the Low Folded Zone according to (Dunnington, 1958) or zone of Hamrin – Makhul according to Buday and Jassim (1987), which it is an Unstable Shelf Zone. Structurally, the oil field is representing an asymmetrical sinusoidal elongated anticline which extending about 40km in length and 3.5km in width between Kirkuk and Qara Chuq anticlines (Figure 1). The southern limb of the structure is steeper and its slope about (37°-65°) while the eastern limb slope is about (22°-35°) (Buday, 1980).

The field consists of two domes are Dauod and Kithka Domes which separated by saddle called Shahal saddle with general direction southeast – northwest. The dome of Kithka is characterized by bigger distance and its structural height (335m) than the dome of Dauod.

Mahdi et al., (2022a) studied the microfacies and diagenetic analysis for Late Oligocene-Early Miocene succession in the Khabaz oil field, and then they studied the structural analysis for this succession in the same oil field (2022b).

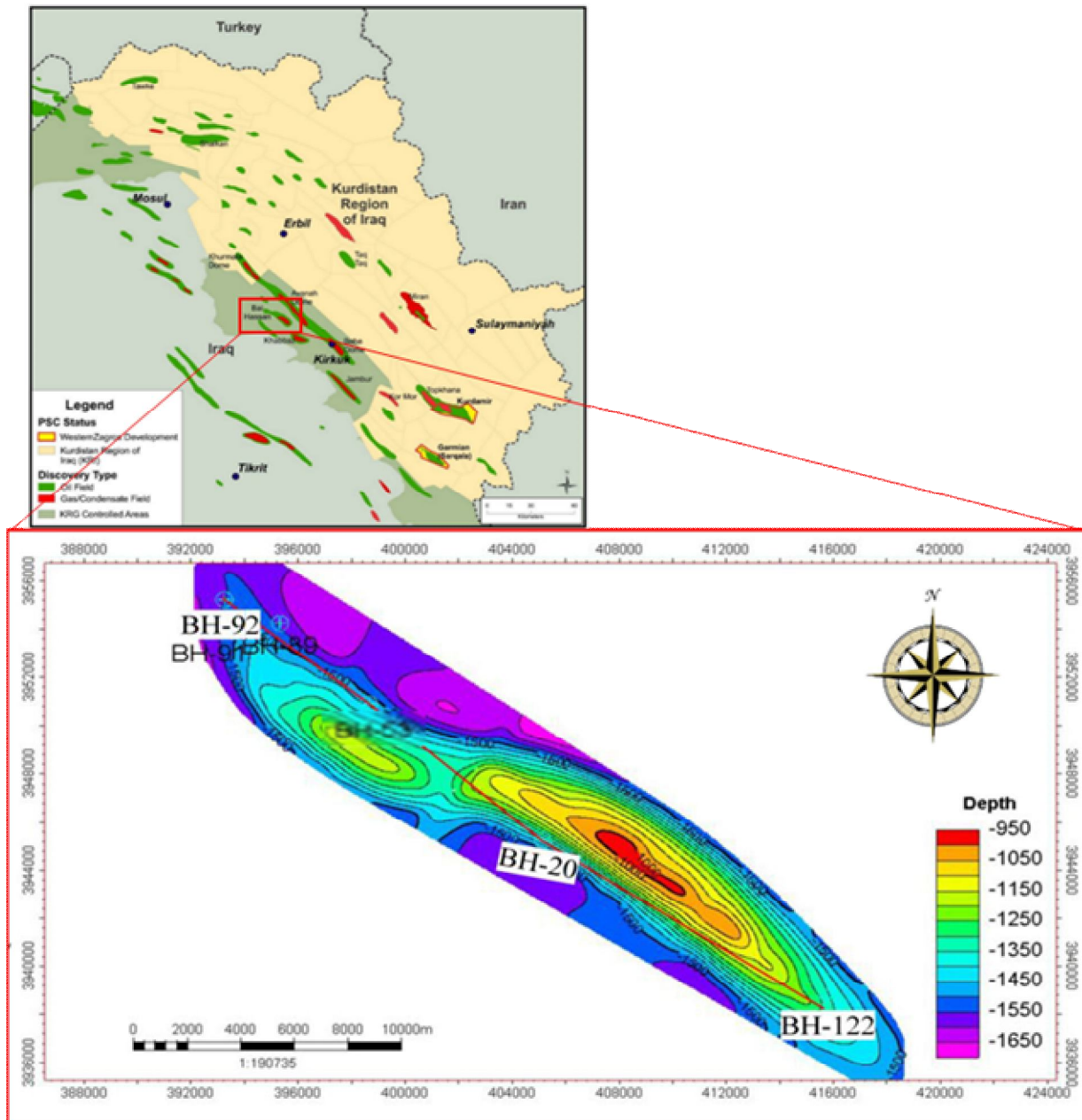


Figure 1: Location and structural map of Bai-Hassan oil field.

## **2. MATERIALS AND METHODS**

In the present study, several types of well-logs obtained from BH-20, BH-39, BH-53, BH-89, BH-91, BH-92, and BH-122 wells which including gamma ray (GR), neutron (NPHI), density (ROHB), sonic (DT), spontaneous potential (SP) and resistivity (LLD, MSFL) well-logs were used in order to determine and study of reservoir characterization to explain different parameters including lithology with contacts identifications, total (PHIT) and effective (PHIE) porosities, permeability, water saturation (SW) and hydrocarbon saturation (Sh), of Oligocene succession in the Bai Hassan oilfield within Zagros basin, northern Iraq. These elements have been accomplished through the following:-

- 1- Made Quality-check (QC) for the primary data including (processing, and arranging it according to the formats there required in the software used.
- 2- Study the available well logs and relate the log response to petrophysical property changes.
- 3- Calculation of the petrophysical properties (Logs Interpretation) from the collected well logs by Techlog software and suggest the electro facies to correlation with limited core data.
- 4- Preparing 2D and 3D geological models for Oligocene reservoir including (Horizon mapping as depth and thickness for reservoir units, petrophysical characteristics distribution) by using Petrel software (Schlumberger Technology).

## **3. GEOLOGICAL SETTINGS**

### **3.1 Tectonic Settings**

The Arabian Plate Megasequence eleven (AP11) is deposited with the Neo-Tethyan terrain collision along eastern and northern sides of the Arabian Plate, which resulted in folds and thrust systems of the Neo-Tethys terrain.

The Aden Gulf and the Red Sea opening, associated by thermal tectonic uplifting, basalt flooding, and tectonic rifting in the southern and western parts of the Arabian plate. The Aden Gulf was opened at the first stage during the Oligocene period, and then during the second stage the Red Sea was opened during the Early Miocene (Hughes and Bydoun, 1992).

There are many tectonic classifications of Iraq, one of them according to Buday, (1980) where divided Iraqi terranes tectonically into three tectonic zones: Stable Shelf, Unstable Shelf and the Imbricate Suture (Zagros) zones (Figure 2). The Central Zagros Faulting Zone is characterizing by high thickness of the sedimentary cover (more than 13 km in thickness), in addition to well development of the folding which formed by long, narrow with northwest – southeast trending anticlines which separating by the broads, flats synclines. There are many presences of major oil fields in this area, which are the Kirkuk, Bai-Hassan, and Jambur (Verma et al., 2004).

Bai-Hassan oil Field is representing asymmetrical double-plunge elongated anticlines, that characterizing the Low Folded Zone within Unstable Shelf Zone in the northeastern-eastern parts of Iraq. The north west to south east structure trending which measures about 34 km in length and 3.5 km in width. The dip angles on the flanks of the structures are about 40° and the dip value of the plunging about 5°. Dip-meter well log data from these wells are showing local dip values more than 50° that are most likely association with the fault systems (Buday and Jassim, 1987).

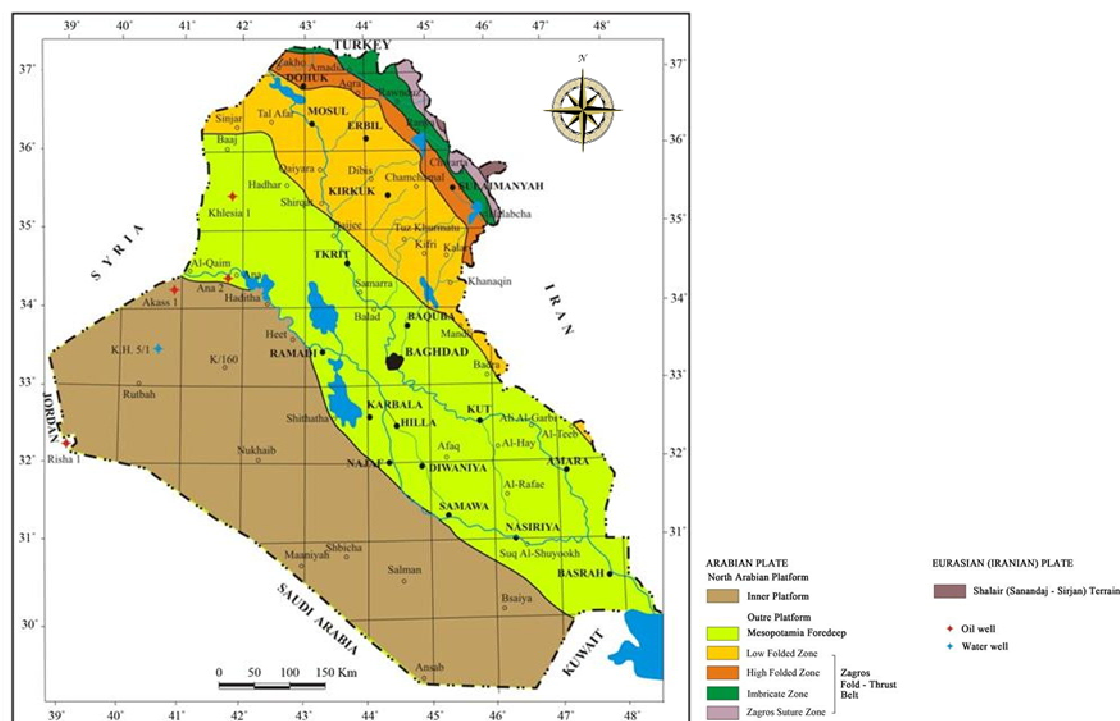


**Figure 2:** Tectonic map of Iraq (Fouad, 2012).

These domes of Bia-Hassan are topographically separating by Shashal-Saddle. It is high like that the Shashal Saddle is associating with deep seated, perpendicular axis, faults extensions were reactivated and influenced in the general evolution of the of Bai-Hassan structure during the Miocene folding and compression stage. This structure is still compressing until today (Buday and Jassim, 1987).

Two distinctive tectonic periods are contributed the creations of the present-day structures and resulting the stratigraphic setting. Early tectonic stage pre the rifting during the Tertiary period caused by the collision of the Arabian Plate with Eurasian Plate which generated the graben systems of the normal faults and faulting of the basement blocks that were covering with high thickness sediments of the carbonate platform.

The early compressional Tertiary stage was resulted in closure and shallowed of the ancestral sea-way of the Cretaceous (Buday and Jassim, 1987).

### 3.2 Stratigraphic setting

Kirkuk Group is representing of major parts of the carbonate succession (mid-upper Eocene to Oligocene). Main limestones term is referred to an informal nomenclature which identified the first mainly oil pay zone in Kirkuk structures. 9 formations of Oligocene succession are observed within Kirkuk Group (Figure 3) that appears in structure of Kirkuk (Bellen et al, 1959 and Al-Naqib, 1960) are; Shurau, Sheikh Alas, Palani, Bajawan, Baba, Tarjil, Anah, Azkand and Ibrahim formations in one stratigraphic package. The absence of the certain Kirkuk group successions may reflect the paleo configurations of the sedimentary basins (Majid and Veizer, 1986).

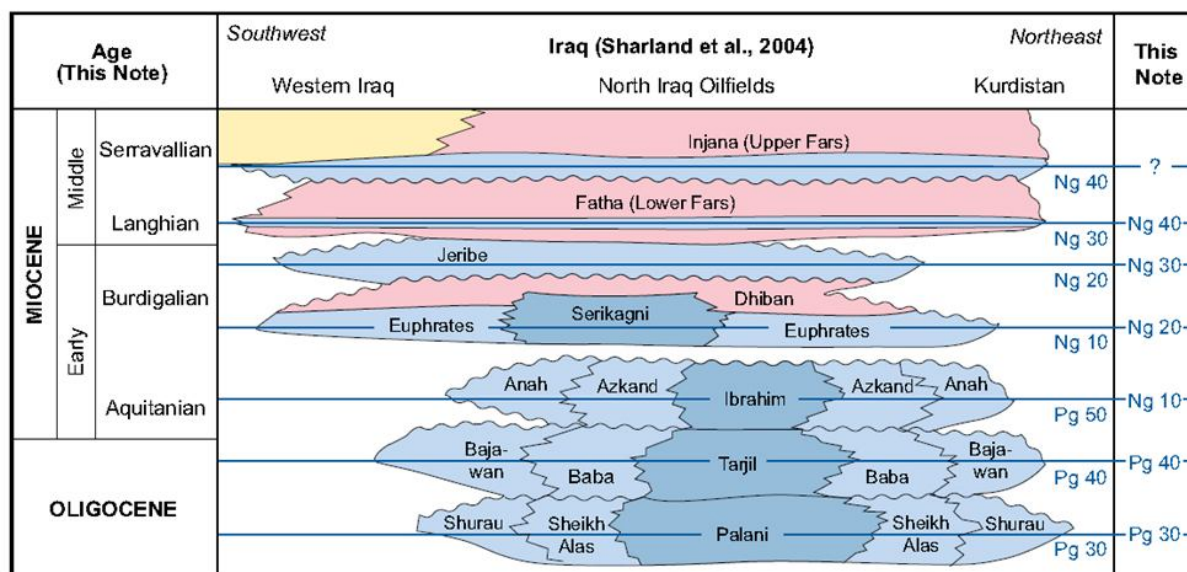


**Figure 3:** Stratigraphic section showing the Tertiary sequence of Iraq appeared the natural of the contact (modified after van Bellen et al., 1959 by Al-Banna, 2008).

Tertiary succession are the most widespread deposit on the outcrops and in the subsurface sections throughout almost all the structural and tectonic parts of Iraq. However, Tertiary rock units have a small area extent in the High-Folded Zone, Imbricated Zone and northern part of Thrusting Zone unit (Ghafur, 2012). The studied successions are characterized by various facies, and including typically eugeosyncline sediments, molasses and platform cover sediments. The Tertiary succession can be divided into individual depositional cycles. Ditmar et al. (1971) situate the contact between the two main evolution stages of Iraq on the early and middle Eocene boundaries, considering the middle Eocene to Quaternary periods as on thicker sedimentary cycles, corresponding to the late and post-geosyncline tectonic development stage. The Oligocene Epoch is marked by uplifting and first-stage of folding during Tertiary eugeosynclinal phase and by a well-expressed regression phase on the shelf setting.

Bellen (1956) suggested a tripartite horizontal and vertical divisions, claiming the present of early, middle and late Oligocene, each of them is

characterized by three facie associations i.e., back-reef / reef, fore-reef and deep basinal facies, back-reef / reef Bajawan succession and fore-reef Baba succession which was introduced by Bellen (1956) and Bellen et al. (1959), the Shurau, Sheik Alas, and Palani successions are represented the early-stage of Oligocene. Baba, Bajawan and Tarjile successions are represented middle stage Oligocene and Anah, Azkand and Ibrahim successions of Early – Late Oligocene (Figure 3).

The Baba succession is consisting of bioclasts, dolomitic limestone, this formation is characterizing by the dominance of large foraminifera such as Lipidocyclina, mollusca, and echinoderm (AL-Hashimi and Amer, 1985). The Bajawan formation was explained by Bellen (1956) it consists of tight back-reef miliolids limestones which alternating with porous dolomite unit. The upper contact is unconformity surface with overlaying Fatha conglomerates. While the lower contact is representing a conformable surface with underlying Shurau succession in Kirkuk Oil Field, except K-152 where the contact is unconformable with Tarjil succession.



Henson (1950) in Jassim and Goff (2006) suggested that the original stratigraphic setting and the reefal concepts (back-reefs, reef, fore-reef and basinal association facies) for the Oligocene succession in Kirkuk Oil Field. It has been revised by Buday (1980) where suggested that sequence of Oligocene was bounding by the non-depositional and/or unconformity surfaces at both its lower and upper boundaries. It would be sited within the first succession of Arabian Plate Mega-sequence eleven (AP110 and Neogene ten (Ng10) (Jassim and Goff, 2006).

The successions were showed lateral variations of facies from the basinal to reef and back-reef association facies. Dittmar with soviet team (1971) were modified the Bellen's subdivisions into two sequences only rather than three sequences according to the lithologic variations and well-logging correlation; they arrangement the Oligocene formations into two successions: the lower succession is comprised of Palani, Sheikh Alas, Shurau and Tarjil Formations and the upper succession is consisting of the Ibrahim, Anah, Azkand, Bajawan and Baba Formations

#### 4. SHALE VOLUME ESTIMATION (Vsh)

A gamma-ray (GR) log is an indicator of the radioactive materials in geological formations. As a result, the log can be used to find and assesment radioactive mineral deposits such as potasum or uranium ores (Asquith and Krygowski, 2004). Sharp lithologic breaks consistent with unconformity surface and sequence boundary are often linked to abrupt changes in gamma-ray log response (Krassay, 1998). However, the gamma-ray (GR) log in sedimentary rocks normal reflect the shales contents of these sediments, because the radioactive elements tending to concentrate in clay and shale. Furthermore, clean rock units generally have a minimum concentration of radioactive ratios, unless the radioactive contaminantion such as volcanic ash or granitic wash is present or waters of formation contain dissolving radioactive salt (Darwin V. Ellis, 1989; Schlumberger, 1972). Gamma ray well logs can be using to calculate volum of shale in the porous reservoir units because shales are usually more radioactive than sands or carbonates.

In this regard, this log has been considered as a direct indicator for shale volume, the low values response of gamma ray indicates the clean units intervals. In order to reveals interval units with better reservoirs probability, the shale volume in the Oligocene carbonate succession has been estimated from a gamma ray well log, in the first step gamma ray index was obtained using Larionov, 1969 equation (1). While a second-step determination of shale volume is the linear response. These methods are summarized in equations 1and 2:

$$I_{GR} = \frac{GR \log - GR \min}{GR \max - GR \min}$$

$$V_{sh} = 0.33 * (2^{2 * I_{GR}} - 1)$$

I GR: gamma-ray index

GR log: gamma-ray reading of gamma-ray lof of the formation

GR min: minimum gamma-ray (for clean sand bed or carbonates)

GR max: maximum gamma-ray (for shale beds)

Tarjil Formation has the lowest Vsh values, ranging from 0.0001 to 0.2515, while Palani Formation shows the highest shale volume trends ranging from 0.0298 to 0.999, with a peak values in the BH-53 well deeper zone of Palani Formation, which has the highest shale volume compared to the other formations. The Baba Formation and Bajawan Formation show similar shale volume trends that range between 0.006-0.91 and 0.006-0.75 respectively, suggesting that these formations contain a very low level of radioactive materials except for some zones of Palani and baba formations, which Vsh values reached up to 0.90 of Vsh. This could be due to the presence of radioactive contaminants such as clay minerals, or the availability of dissolved radioactive salt in formation waters (Ellis and Singer, 2008).

#### 5. POROSITY ASSESMENT

Porosity is the volume of pore of for the reservoir rocks that filled and yields hydrocarbon or water (Cluff and Cluff, 2004; Hook, 2003; Rider and Kennedy, 2011; Shepherd, 2009). The porosities fraction of reservoirs is described as the void or pore space fractions of the rock, which represents

the ratio of the pores volume to the rocks bulk volume. Porosity is generally expressed as a decimal fractions or as a percentages and it's usually representing by the Greek letter phi ( $\Phi$ ) (Eq.3). Moreover, the porosity of carbonate reservoir rocks ranges between 1-35% with an average of up to 10% in dolomite reservoir rocks and up to 12% in limestone reservoir rock units (Schmoker et al., 1985). In the present study, The porosity prediction is characterized by the neutron, density, and sonic well-log parameters.

$$\text{Porosity } (\Phi\%) = (\text{Pore volume})/(\text{Bulk volume}) \quad (3)$$

However, a single porosity well-log parameter such as sonic, density, neutron logs, or a combination of several type of porosity well loggings can be using in order to determination of the porosity values and to avoid different lithology effects on these values (Doveton, 1994).

### 5.1 Density Porosity

The density well log is a useful tool to lithologic discrimination as well as to calculate the porosities and hydrocarbons densities. The general interval scale for this measurement is from 1.95 to 2.95, with units of g/cm<sup>3</sup> (Rider and Kennedy, 2011). The general equation (4) to measure the porosity expressed by Rider and Kennedy (2011) as follow:

$$\Phi_p (\text{PHID}) = ((\rho_{ma} - \rho_b)) / ((\rho_{ma} - \rho_{fl})) \quad (4)$$

Where:

PHID = Porosity derived from density log

$\rho_{ma}$  (RHOB ma) = Density of the materials matrix (Ss = 2.65 g/cc, Ls = 2.71 g/cc, dolomite = 2.87 g/cc)

$\rho_b$  (RHOB) = General log reading of rock density

$\rho_{fl}$  (RHOB f) = Fluid density (fresh water mud = 1.0 g/cc, salt water mud = 1.1g/cc).

In the cases where shale volume is reached values more than 10%, the following equation is used to correct the density porosity (Dresser Atlas, 1979; Tiab and Donaldson, 2015, 2004).

$$\Phi_{Dcorr} = (\rho_{ma} - \rho_b) / (\rho_{ma} - \rho_{sh}) - V_s (\rho_{ma} - \rho_{sh}) / (\rho_{ma} - \rho_{fl}) \quad (5)$$

The density porosity on BH-20, BH-53, BH-122, BH-89, BH-91, BH-92, BH-39 wells revealed that both Bajawan (-A) and Baba (B) formations have

the highest porosity values reaching up to 0.51. while the data from Tarjil (BE) Formation showed that the porosity values range from 0.13 to 0.28 and the lowest porosity values have been recorded for the Palani (E) Formation, which reached up to 0.18.

### 5.2 Sonic Log

The porosity of the rock unit could be established by measured its acoustic velocities by the sonic well logging, in other words, the acoustic tool measures the transit interval time (t) or the time in microseconds for an sonic waves to travel through 1 foot or 1 meter of a rock unit along a path parallel to the boreholes, which can be using to porosity calculation (Selley, 1998). The boreholes compensated (BHC) devices were using in the Bai-Hassan oilfield and the Wyllie time average equation was utilized in order to measure the porosity from the sonic well log as follow:

$$\Phi_S = (\Delta t_{log} - \Delta t_{ma}) / (\Delta t_{fl} - \Delta t_{ma}) \quad (6)$$

Where:

$\Phi_S$  = Sonic-derived porosity.

$\Delta t_{ma}$  = interval transit time in the matrix ( $\Delta t$  limestone is used)

$\Delta t_{fl}$  = interval transit time in the fluid in the formation (freshwater mud = 189  $\mu\text{sec/ft}$ ; saltwater mud = 185  $\mu\text{sec/ft}$ ), based on the type of drilling mud used in each well.

$\Delta t_{log}$  = interval transit time in the formation (measured by log).

The transit interval time ( $\Delta t$ ) of the evaluated rock unit is increasing due to the presence of the hydrocarbon (i.e., oil or gas) and decreases as a result of shale increasing in the bedrocks. If the effects of hydrocarbon are not corrected, the sonic obtained values of porosity will be too high. In this regards, Hilchie (1978) suggested the following empirical correction for the hydrocarbons effects:

$$\text{For gas-bearing zones: } \Phi = \Phi_s * 0.7 \quad (7)$$

$$\text{For oil-bearing zones: } \Phi = \Phi_s * 0.9 \quad (8)$$

The porosity values from the sonic log showed the same conclusions as obtained from neutron and density porosity data, where sonic porosity for Bajawan (-A) and Baba (B) formations reached up to 0.37, the Tarjil Formation has porosity values of up to 0.24.



## 6. TOTAL AND SECONDARY POROSITY

The primary or total porosities are the amounts of pores which present in the sediments at the deposition time or formed during the sedimentation. It is usually a function of the value of space between the rock forming grains. The porosity from sonic log is representing the primary porosity (intergranular) (Asquith and Gibson, 1982).

While the secondary type of porosity (vuggy, moldic, channels, and fracture) is formed from geological processes such as diagenetic processes after the deposition (Tiab and Donaldson, 2004). The secondary type of porosity index (SPI or PHIE) may be calculated as the difference between the total porosity as determined from Neutron and Density well logs with porosity data acquired from sonic (DT), by applying the following equation (Schlumberger, 1972).

$$PHIE = \Phi_{N.D} - \Phi_s \quad (9)$$

where :

PHIE = secondary porosity index

$\Phi_{N.D}$  (PHIT)= neutron-density derived porosity

$\Phi_s$  = sonic-derived porosity.

The total porosity is calculated from the density and neutron logs, by using this equation (Doveton, 1994; Schlumberger, 1989).

$$\Phi_{N.D} = (\Phi_N + \Phi_D) / 2 \quad (10)$$

In the case of the  $\Phi_N < \Phi_D$  the root is used in the same equation (Bowen, 2003). this equation can be applied in order to obtain the corrected porosity value from the gas effect (Bassiouni, 1994).

$$\Phi_{N.D} = \sqrt{(2\Phi_N + \Phi_D) / 2} \quad (11)$$

Or by using the following equation:

$$\Phi_{N.D} = 1/3 \Phi_N + 2/3 \Phi_D \quad (12)$$

Histograms of the total and effective porosity model on the BH-20, BH-53, BH-122, BH-89, BH-91, BH-92, BH-39 wells show that the Bajawan and baba formations have the highest data frequency, between 0.002- 0.39 and 0.002- 0.274 and 0.0001- 0.33, and 0.02-0.28 respectively. Similarly, the data from Baba Formation ranges from 0.04 to 0.28, and of up to 0.25 for Palani Formation.

## 7. EFFECTIVE POROSITY MODELS

The Effective porosity express the volume ratio of interconnected pore-space to the total of a porous samples. Its importance comes from control on the magnitude of fluids Flow, therefore its play big role in the evaluation of recoverable hydrocarbon (Moradi et al., 2016), the effective porosity of carbonate reservoir affected by facies distribution, diagenesis imprint and situation of within any study area. There are several methods for measuring Effective porosity now the method used in the current study relies on the equation described in Zughar et al., 2020, these equations are :

$$Q_t = \sqrt{Q_n^2 + Q_D^2} / 2 \quad (13)$$

$$Q_e = Q_{total} \times (1 - V_{sh}) \quad (14)$$

$Q_t$  = total porosity

$Q_n$  = porosity estimated from neutron log (after correction)

$Q_d$  = porosity estimated from density log (after correction)

$Q_e$  = effective porosity

$V_{sh}$  = shale volume

## 8. WATER AND HYDROCARBON SATURATION

Resistivity well logging measurement is usually one of the most important of all well log parameters. Resistance, or the inherent ability to resistant the movement of an electrical current, is present in all materials. It represents the actual measurement of resistance within formations or bedrocks, which is specified as the reciprocal of electrical conductivity (C) and can be expressed as linear formula ( $R_{ohm-m} = 1000 / C$  m.ohm/m).

Resistivity well-logs are primarily used to identify and estimate the concentration of hydrocarbons (oil and gas).

### 8.1 Water Saturation

A coefficient called the formation resistivity factor (F) can be used to link the resistivities of a water filled formation ( $R_o$ ) to the resistivity of the waters (RW) filling the formations (Archie, 1941).

$$R_o = F * R_w \quad (15)$$

Archie (1941) also proved that formation factor (F) can be associating with the porosity of the formation using the following equation:

$$F = a / \Phi^m \quad (16)$$

The water saturation (SW) equation can be represented as follows by combining equations 16 and 17:

$$S_w = [(a \cdot R_w) / (R_t \cdot \Phi^m)]^{1/n} \quad (17)$$

Where:

SW = water saturation

a = tortuosity factor (a = 1.0 for carbonate rocks)

m = cementation exponent (m = 2.0)

n = saturation exponent (n = 2)

R<sub>w</sub> = resistivity of formation water (R<sub>w</sub>)

Φ = calculated porosity values

R<sub>t</sub> = true resistivity as derived from a deep latero-resistivity log (LLD)

Equation 17 is most commonly referring to as the Archie's equation for obtaining water-saturation (S<sub>w</sub>). All of the recent methods that were used in the interpretation regarding resistivity well logs are derived from the Archie equation (Asquith and Krygowski, 2004; Asquith and Gibson, 1982). The LLD does not always recording accurate values for deep resistivity for thin rock unit, resistive layers or zones (were; R<sub>t</sub> > 100 ohm-m). For this reason, an alternating method to calculate true-resistivity (R<sub>t</sub>) values can be used.

The method is known as R<sub>t</sub> minimum, and it is calculating which using the equation below:

$$R_{t \min} = R_i \cdot R_w / R_{mf} \quad (18)$$

Where:

R<sub>i</sub> = resistivity tool which measuring in the invaded zone (Figures 15 and 16), usually laterolog or spherically focused log.

R<sub>mf</sub> = resistivity of mud-filtrate, (R<sub>mf</sub>) = 0.65 ohm-m (Schlumberger, 1972).

The porous and permeable zones are invaded by drilling-fluids, connate waters within formations are displaced by mud-filtrate. Porosities in water bearing formations can be relating to shallow-resistivity (R<sub>xo</sub>; Figsure 4 and 5) and can be represented as the following equation:

$$S_{xo} = [(a \cdot R_{mf}) / (R_{xo} \cdot \Phi^m)]^{1/n} \quad (19)$$

S<sub>xo</sub> = water saturation in the flushed zone

R<sub>xo</sub> = flushed-zone resistivity

In this regard, several parameters should be determined in order to estimate water and hydrocarbon saturation, such as R<sub>mf</sub>, R<sub>w</sub>, T<sub>f</sub>.

## 8.2 Formation water resistivity (R<sub>w</sub>)

Formation resistivity measurement represents one of the main components utilized to determine the fluid saturation in reservoir rocks. It is a function of the porosity and fluid type (hydrocarbon, fresh, and/or saltwater), as well as the rock type, where all of the rocks and hydrocarbons are working as an isolator. While the saltwater connected, and the resistivity measurements that are made by logging equipment could be using to determine the presence of hydrocarbon and calculating the porosity of the reservoirs and because of the movement of fluid during the drilling of the well through the formations with porosity and permeability surrounding the borehole resistivity measurement recording at different depths in the rock unit we often have different values (Zhang et al., 1999).

$$R_w = R_{ws} \times ((T_s + 21.5) / (T_f + 21.5)) \quad (20)$$

Where:

R<sub>w</sub> = formation water resistivity at formation temperature

R<sub>ws</sub> = formation water resistivity at surface temperature.

Relations among petrophysical parameters, hydrocarbon occurrence, and the lowest values of water saturation with thier correlation (4 and 5).

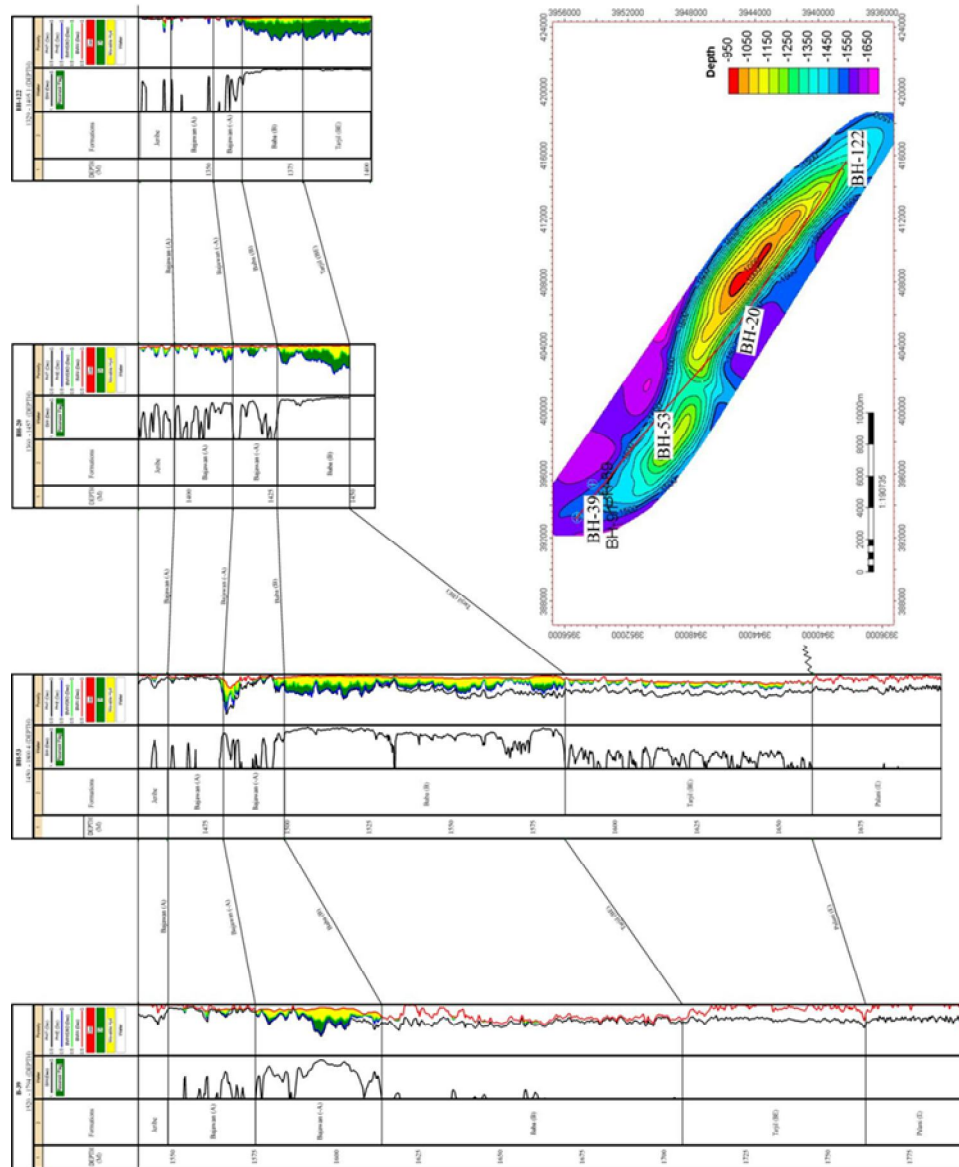


**Figure 4:** Petrophysical 2D correlation model of well BH-39,53,20 and 122, showing petrophysical, shale volume, total, effective porosity, and water saturation model.

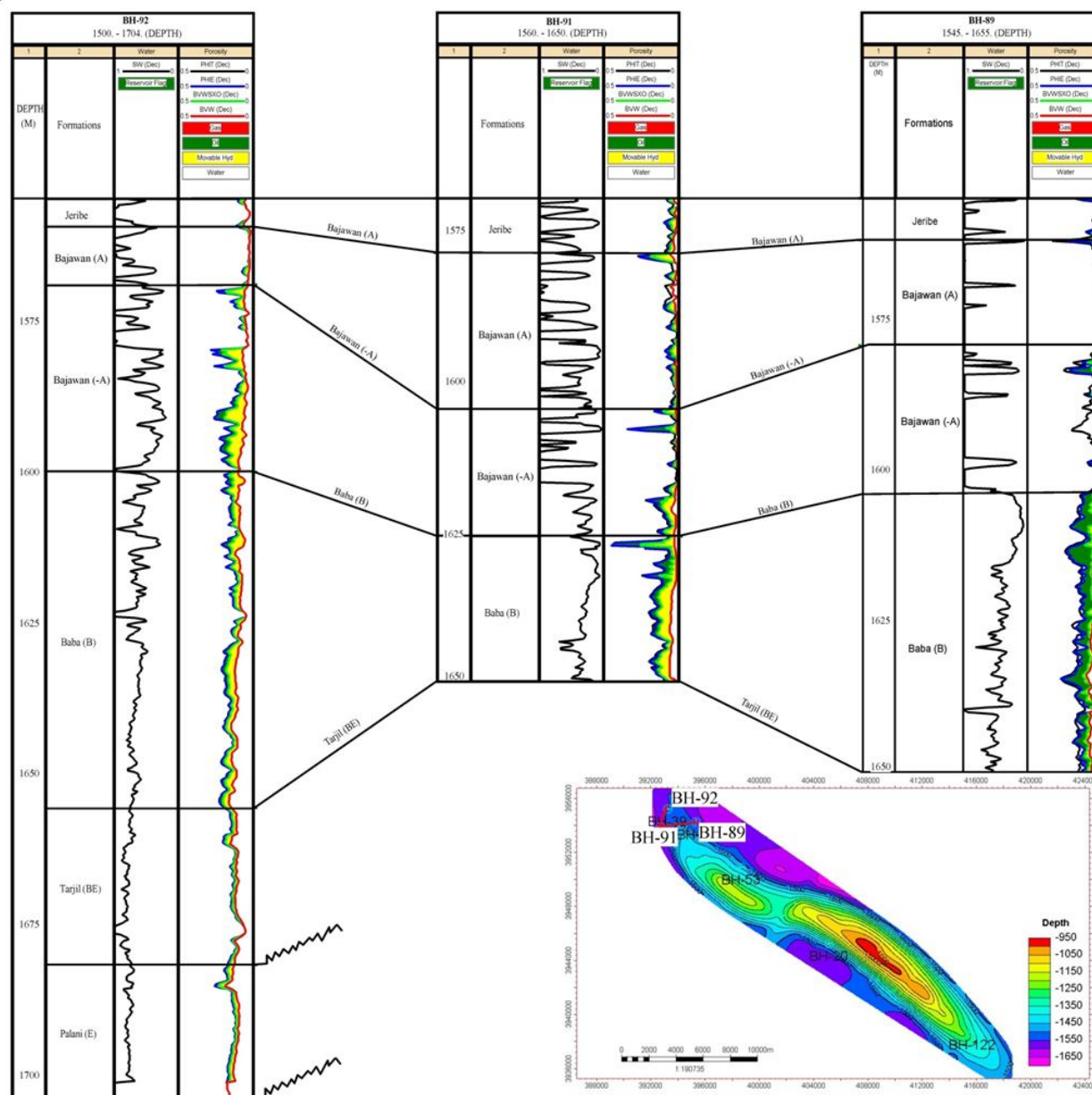


**Figure 5:** Petrophysical 1D correlation model of well BH-89, 91 and 92, showing petrophysical, shale volume, total, effective porosity, and water saturation model.

## 9. PERMEABILITY MODEL

The logs derived permeability (K) formula are only valid for estimated the permeability in any rock units must be at irreducible waters saturation (Swirr) (Schlumberger, 1977; in Asquith &

Krygowski, 2004), therefore before calculating the permeability for studied formation we must first determined whether or not the studied formations are at Swirr. The Knowledge of the current study rocks are within the Swirr depends on the bulk

volume water values and this can be estimated through the following equation:

$$BVW = S_w * \Phi. \quad (27)$$

(Asquith & Krygowski, 2004)

When the BVW values of study formation rocks are constant, the zone is at  $S_{wirr}$ .

### 9.1 Constant calculating

The Zone at constant BVW estimation for fixing the  $S_{wirr}$  need to estimation the constant of following equation:

$$\text{Log } S_{wirr} = \text{Log constant} - \text{logy } \Phi \quad (28)$$

(Timur, 1968)

It's important to clear that the  $\Phi$  represent the  $\phi_e$  the constant estimation of studied Bai-Hassan

oilfield through choosing two representatives well, the well BH-20 represent the Kithka dome area, while the well BH-53 represent the Daoud dome. The available data (appendix A) used to draw (Log - Log graphs between Log  $\phi$  and Log  $S_w$  for both wells, the intercept values equal that read from the figures (6) and (7) are equal to 0.05 and 0.04 at both well BH-20 and BH-53, represent the constant values respectively, these values were used to calculate the values of the Permeability in each of the two studied wells BH-20 and BH-53 through using the following formula:-

$$K = [79 \times (\Phi^3 / S_{wirr})]^2 \quad (29)$$

(Timur, 1968) The  $\Phi$  in this formula represent the  $\phi_e$ .

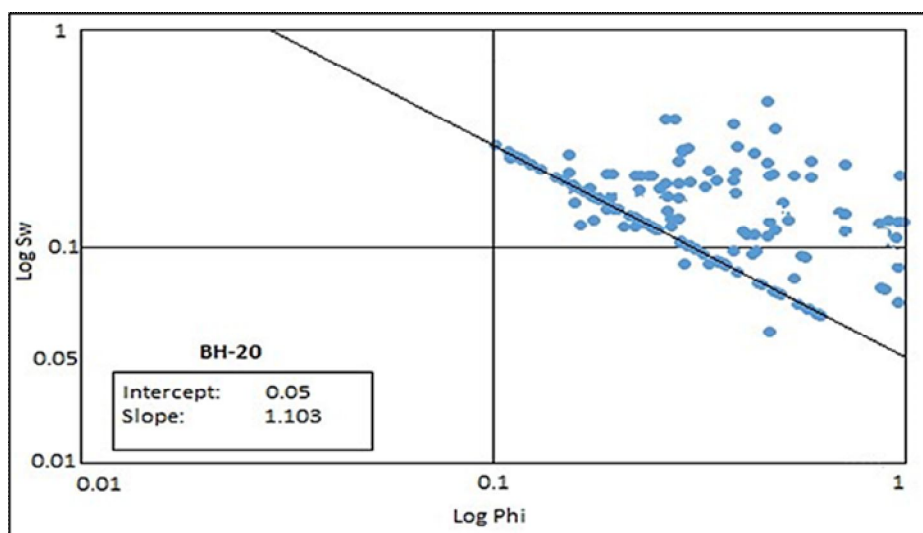


**Figure 6:** Log - Log graphs between Log  $\phi$  and Log  $S_w$  for BH-20 wells.

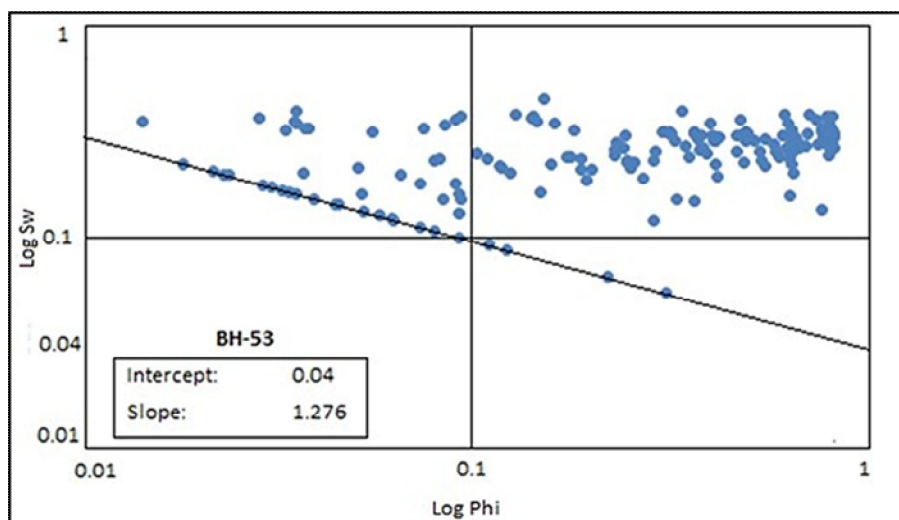


**Figure 7:** Log - Log graphs between Log phi and Log Sw for BH-53 wells.

The obtained permeability values represent the Predicted values, therefore these values need to be corrected by comparing them with values calculated from the core samples, and due to these values are available only in wells BH-20 and BH-53, they have been treated statistically (by using SPSS Software) in order to obtain a constant value for both well which were represent the two domes of Bai-Hassan oil field, and used it in the correction processes for the values that were

calculated in all studied wells through logs. The figures (8, 9) reveal the comparison between log derived permeability and calculated from core samples. The correction process included all the formation that appears in the two wells BH-20 and BH-53, in order to obtain an accurate result when constructing the 3D model of the cumulative accumulated permeability which comprehensive all studied formation within all studied wells.

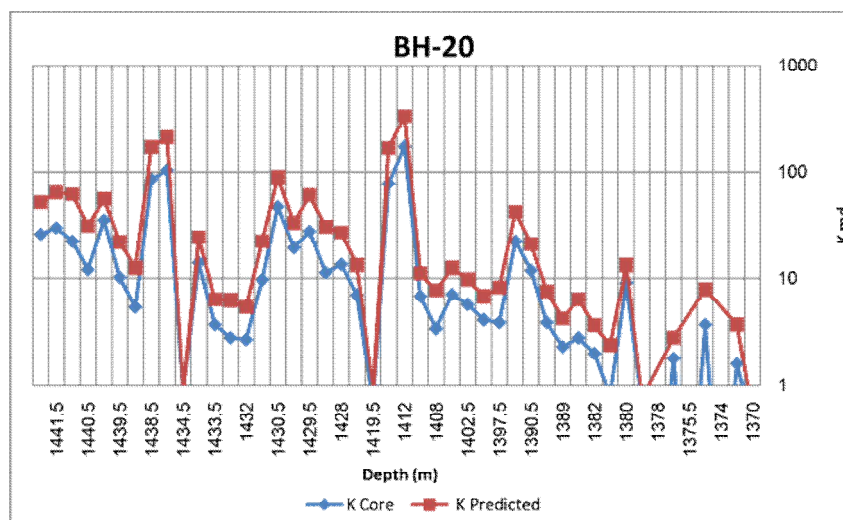


**Figure 8.** Comparison between log derived permeability and calculated from core samples for BH-20 wells.



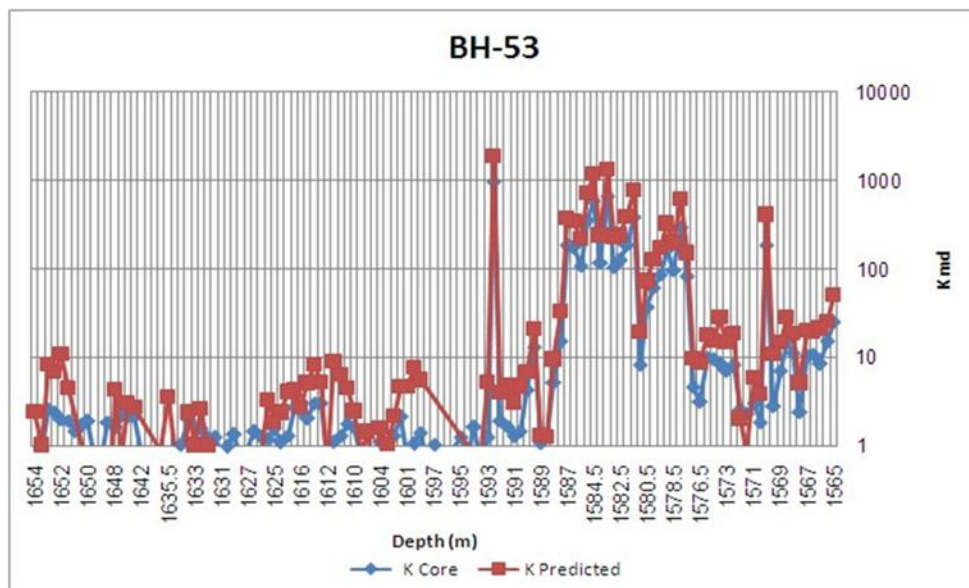


**Figure 9:** Comparison between log derived permeability and calculated from core samples for BH-53 wells.

The result of the statistical analysis revealed the existence of an excellent Correlation coefficient (R) between the permeability values calculated (predicted) from well logs & those obtained from core samples, the R value were equal to 0.978 and 0.994 in the both presentative well BH-202 BH-53 respectively. Depending values of R two formula were obtained to permeability correction the predicted values within the all studied well, these formulas are as follow:-

$$K_{core} \text{ BH-20} = (\text{Predicted K} * 1.040) - 3.363 \quad (30)$$

$$K_{core} \text{ BH-53} = (\text{Predicted K} * 1.030) - 3.359 \quad (31)$$

The cumulative model of the permeability (Figure 10) shows that the permeability ranges from fair

to very good, with the exception a very small spot at the extreme southeast of Kithka dome, and that its better distributed in the rest of the other areas on the some of Kithka dome compared to the dome of Daoud rest. The reasons may be that the sedimentary basin was as we previously explained more deeper toward Daoud dome area, this fact obtained through the volume of shale which was higher toward the Daoud dome area, as well as the other reason is the recurrence of diagenetic processes due to instability at the study area (Al - Jwaini & Gayara, 2016; Sadooni & Alsharhan, 2019).

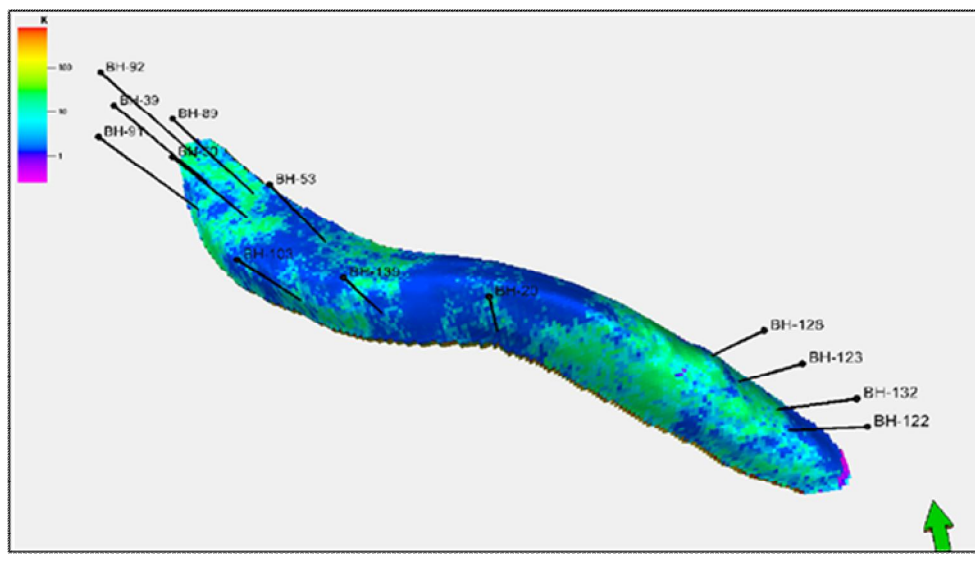


**Figure10:** 3D cumulative accumulation permeability distribution model in the studied formations, Bai-Hassan oil field.

## 10. HYDROCARBON SATURATION

Fluids saturation property expressing as the fractions or percentages of the total volume of pore occupied by the oil, gas, or water (Tiab and Donaldson, 2004), the hydrocarbons saturation can be deduced by the following relation.

$$S_h = 1.0 - S_w$$

Hydrocarbon saturation term ( $S_h$ ) gives good data related to productions. Also, a comparison of  $S_w$  and  $S_{xo}$  in a hydrocarbons zone is considering to give movable hydrocarbon, so the difference between the waters saturation of flushed-zone ( $S_{xo}$ ) and the original uninvaded-zone waters saturation ( $S_w$ ) is equal to the fractions of movable hydrocarbon in the rock unit. Furthermore, hydrocarbon saturation includes either movable and residual hydrocarbon saturation. Recoverable (movable) hydrocarbons represent producible hydrocarbons, while the residual hydrocarbons are left in reservoirs and cannot be produced (Bates and Jackson, 1980).

$$MOS = S_{xo} - S_w$$

$$\text{Or } MOS = C \left( \sqrt{\frac{R_{mf}}{R_{xo}}} - \sqrt{\frac{R_w}{R_t}} \right) \Phi$$

Where MOS represents Movable oil saturation,  $C = 1$  for carbonate rock

$$ROS = 1 - S_{xo} \quad (21)$$

Where ROS is Residual hydrocarbon saturation and giving the saturations in unmoved or residual hydrocarbon of the invaded-zone after it is filtrated by the drilling-muds.

In the current study, the porosities are estimating from three well logs; neutron, sonic, and density logging tools utilizing average values of these measurements. Furthermore, shallow and deep resistivities ( $R_{xo}$  and  $R_t$ ) were obtained from LLD and MSFL logs respectively. As it was discussed previously, the two types of data (porosity and resistivity), in addition to other rock unit parameters ( $a$ ,  $n$ , and  $m$ ) were using to calculate

the formation waters saturation ( $S_w$  and  $S_{x0}$ ) and BVW.

In this regards, water saturation was multiplied by the porosities to represent it as volume fraction occupying the porosity:

$$BVW = S_w * \Phi \quad (25)$$

$$BVWS_{x0} = S_{x0} * \Phi \quad (26)$$

The first quantitative perception as a conventional hydrocarbon reservoir quality of carbonate rocks, in terms of their petrophysical properties in the Bai Hassan oilfield, Zagros basin, demonstrates the existence of intervals with favorable characteristics to accumulate hydrocarbons, represented in clay volumes  $< 30\%$ , water

saturations  $< 50\%$ , ranges of porosity between  $15\%$  to  $28\%$ . Generally, for hydrocarbon reservoirs, these properties are cataloged as good quality reservoirs according to Shogenov et al. (2015) and with excellent intervals, presenting the most common porosity values in productive reservoirs according to Dikkers (1985).

The cumulative model of  $S_w$  for both Jeribe and upper part of Bajawan formations very small area showed the presence of characterized by little  $S_w$  on the Daoud dome, while the area that represent the Kithka dome characterized by separated patches from  $S_w$ , these patches were occupied large area compared to the Daoud dome area (Figure 11).

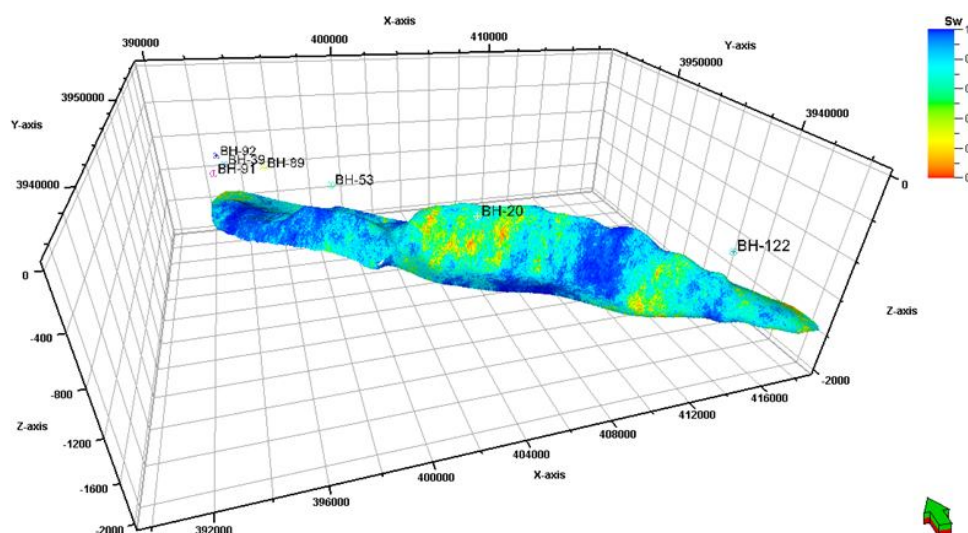


**Figure 11:** 3D distribution model for  $S_w$  within Jeribe-Bajawan (A) formations.

The cumulative model of  $S_w$  within the rocks of Bajawan Formation, the two parts shown a high percent from  $S_w$  in general (Figure 12), with the exception of a limited Patches at Kithka dome area, which was characterize by low percent from  $S_w$ , the reason of these low percent may be the dolomitization effect on the lower part (A) of

Bajawan Formation, while the western part from Bai-Hassan oil field was characterized by deep lagoon deposition. This indicator was recorded through diagnostic the Textularia benthonic foraminifera within the sediment of upper part of Bajawan Formation (see the microfacies part).

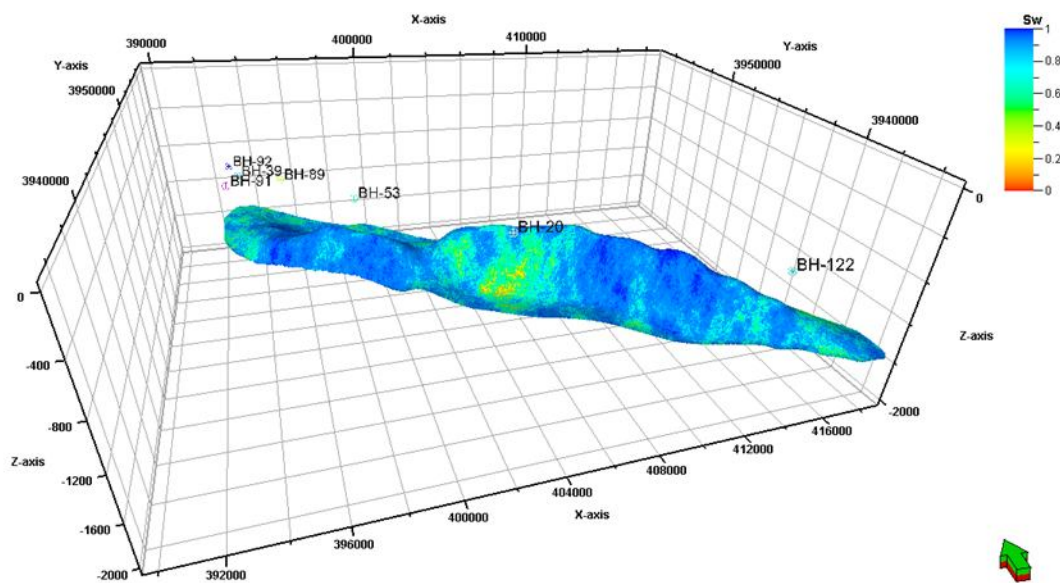


**Figure 12.** 3D distribution model for Sw within Jeribe-Bajawan (A) formations.

The Cumulative model of Sw in the rocks of the lower part of Bajawan Formation with the rocks of Baba Formations (Figure 13) effects an improving of oil reservoir through Low content of Sw occupy large parts from we Kithika dome area, with the appearance of patches from low Sw content at the Daoud dome area.

The Shashal saddle characterize by high content of Sw, which was approaching the value 1. The reason from this different district but of Sw within the rocks of lower part of Bajawan and Baba formations is that the sediments basin was deeper

towards the western. Part from the studied oil field, while the eastern part was less deep, which allowed to reefal facie rocks to growth, the indicate that enhance this idea is the forgoing mod of Vsh and the distinguished microfacies with the studied formations. The figure (14) shows a significant improvement in the petrophysical properties of the reservoir rocks within the Baba and Tarjil formations, because the Sw cumulative model reflect low to very low values, which approach to zero value especially within the Kithka dome area, as well as the Daoud dome area.

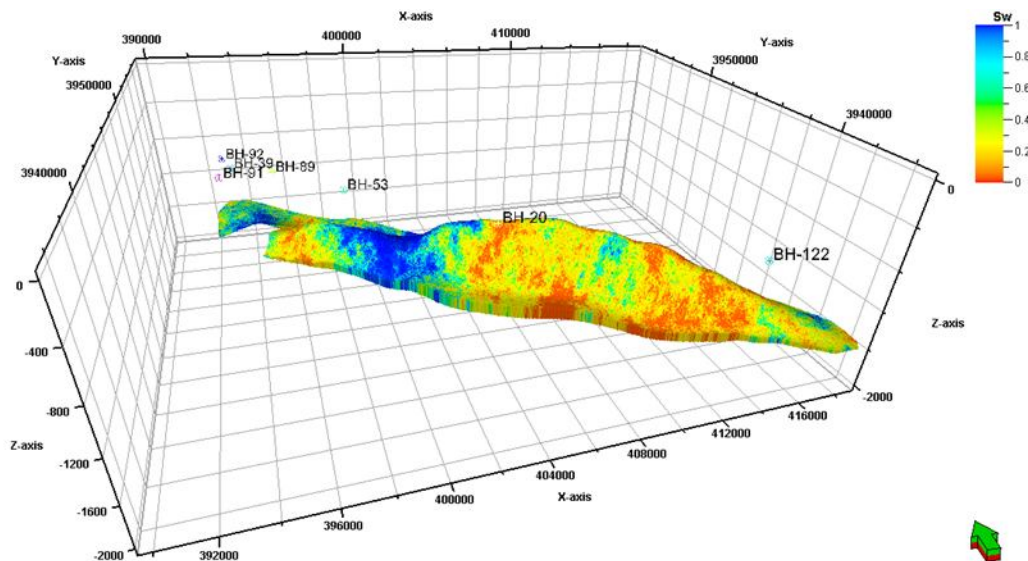


**Figure 13:** 3D distribution model for Sw within Bajawan (-A) - Baba formations.

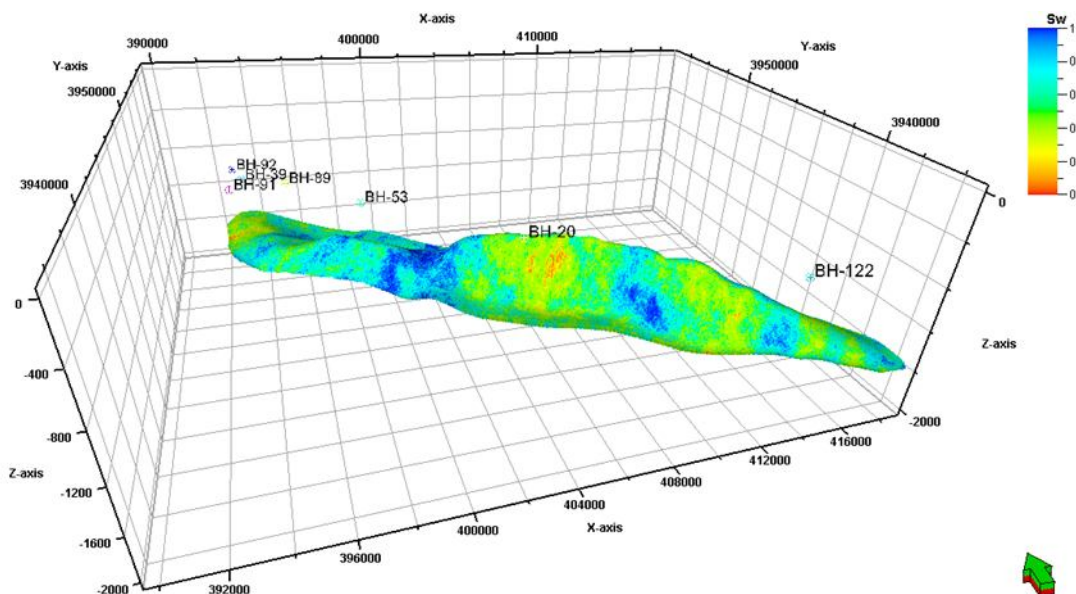


**Figure 14:** 3D distribution model for Sw within Baba - Tarjil formations.

The cumulative Sw model (Figure 15) reveal a significant improvement in the Petrophysical properties with in Tarjil and Palani formation rocks. The improvement was recorded within the Kithka only, while Daoud dome area was characterized by its high content of Sw. Perhaps the reason for this improvement at the eastern part from the studied oilfield with despite the fact that the Tarjil and Palani succession rocks were

deposited in deep marine environment is the effect of tectonic on the studied oilfield through the Miocene epoch (Al - Jwaini & Gayara 2016; Sadooni & Alsharhan, 2019) which led to the rise of the eastern part of the studied oilfield by 335 meters compared to the western part , and this vise of eastern part led to water migrate towards the west where the dome of Daoud is located.



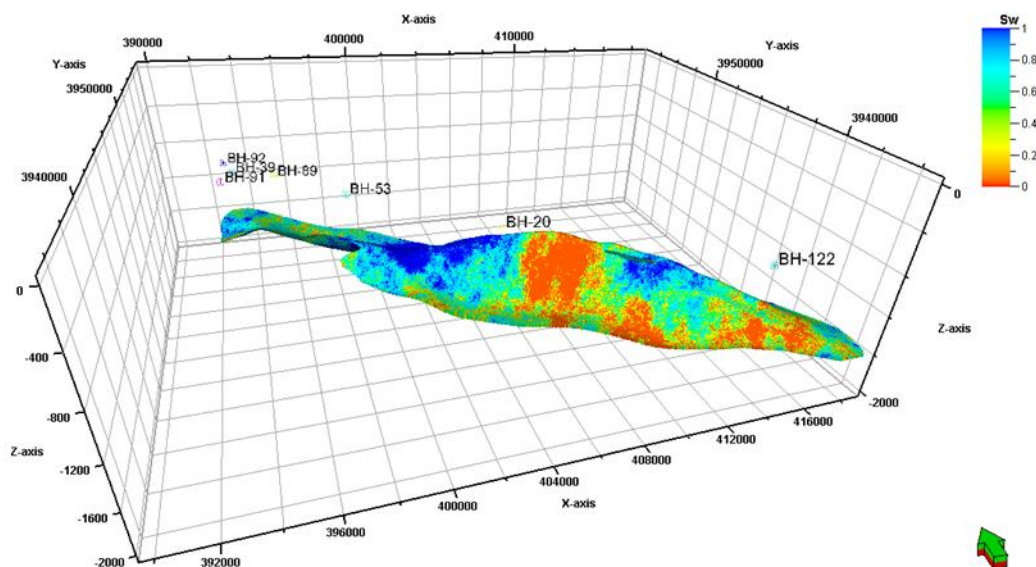


Figure 15: 3D distribution model for Sw within Tarjil - Palani formations.

## 11. MOVABLE HYDROCARBON CUMULATIVE MODEL (MHC)

This cumulative model was made in order to clear (put spotlight) the location of hydrocarbon accumulation (which are movable) within the, and along the Bai-Hassan oilfield, after obtained the all petrophysical parameters which were used at the end to draw the cumulative movable hydrocarbon model

The following equations were used to determine the MHC as a irreducible hydrocarbon saturation ( $S_{hr}$ ) and movable saturated hydrocarbon (MHC) were as follows:-

$$S_{hr} = 1 - S_{xo} \quad (32)$$

(Hamada, 2008)

$$MHC = S_{xo} - S_w \quad (33)$$

The Cumulative model of MHC estimated through substituting all the values for the petrophysical properties as well as the

accumulative thickness of the parts with consideration of the effective Porosity of these parts from the studied reservoir The good reservoir properties are observed in the Bajawan and Baba formations with very little parts from Tarjil Formation. the cumulative model (Figure 16) shows that most of the of oil accumulation are spread as patches over different areas of Kithka dome compared to a small accumulation at the dome of Daoud, this distribution expresses a logical case for many reasons, this reasons and their effects are interrelated with each other , the first effect coming from less affecting of the tectonic subsidence compared with the neighboring Kirkuk oil field, the Bai-Hassan oil field affected by uplift through tectonic operation, and its influence has still continued to Cenozoic (Al-Sheikhly et al. , 2015; Al-Jwaini & Gayara, 2016; Sadooni & Al-Sharhan, 2019). This tectonic effect led to uplift of the Southeastern part from Bai - Hassan oil field by approximately 335m, compared to the northwestern part, due to this



uplift the hydrocarbons have migrated (due to differences in the density) towards the southeastern part, on the contrary, the reservoir waters have accumulated towards northwest under the influence of gravity, which led to the sequestration of hydrocarbon in the small patches within the northwestern part. The continuation of the tectonic effect on the studied formations (rocks) also caused the recurrence of the

diagenetic processes (solution and dissolution) which helped in the presence of effective porosity that Contributed to the migration and accumulation of hydrocarbons, the end effect of tectonic Continuation was the influence on the topography of the basin, this influence was detect through the Vsh which was high at northwestern part (Daoud area), because this part was deeper than the southeastern part (Kithika area).

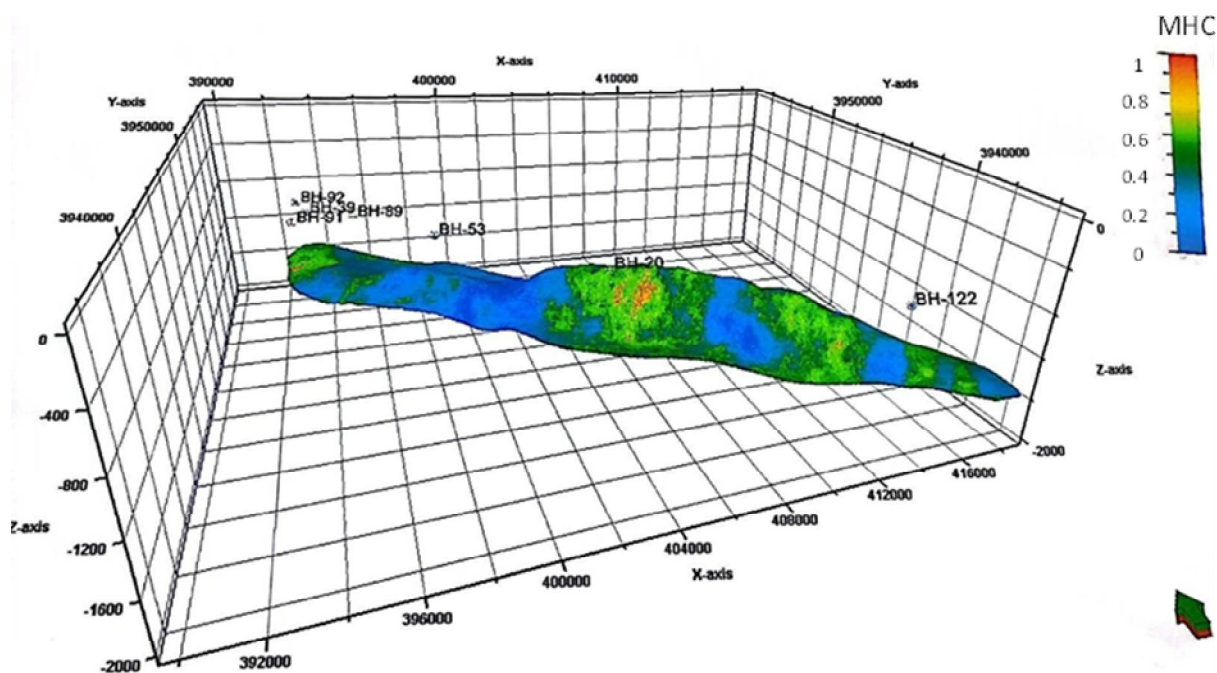


**Figure 16:** 3D cumulative Movable Hydrocarbon distribution model in the studied formations, Bai-Hassan oil field.

## 12. CONCLUSIONS

In the current study, several types of well-logs obtained from BH-20, BH-39, BH-53, BH-89, BH-91, BH-92, and BH-122 wells are including gamma ray (GR), neutron (NPHI), density (ROHB), sonic (DT), spontaneous potential (SP) and resistivity (LLD, MSFL) well-logs were used in order to determine and study of reservoir characterization to explain different parameters including

lithology with contacts identifications, total (PHIT) and effective (PHIE) porosities, permeability waters saturation (SW) and hydrocarbons saturation (Sh), of Oligocene succession in the Bai Hassan oilfield within Zagros basin, northern Iraq.

The analysis of the results showed that the Kathka dome area compared to the Dauod dome area is

better in terms of petrophysical properties as well as in terms of its content of hydrocarbon groups.

### **13. ACKNOWLEDGEMENTS**

The authors are very grateful to the reviewers, Editor in Chief Prof. Dr. Salih M. Awadh, the Secretary of Journal, Mr Samir R. Hijab, and the Technical Editors for their outstanding efforts and valuable comments.

### **14. REFERENCES**

1. Albeyati F.M.O.; Abdula R.A.; and Terzi F., 2021. Porosity and Permeability Measurements Integration of The Upper Cretaceous in Balad Field, Central Iraq. *Iraqi Geological Journal*, 54 (1B), pp. 24-42.
2. Al-Hashimi, H.A.J., and Amer, R.M., 1985. Tertiary Microfacies of Iraq. *GEOSURV*, Baghdad, Iraq, 56p.
3. Al-Jwaini Y.S. and Gayara A. D., 2016. Upper Palaeogene-Lower Neogene Reservoir Characterization in Kirkuk, Bai Hassan and Khabaz Oil Fields, Northern Iraq. *Tikrit Journal of Pure Science*, 2016, Volume 21, Issue 3, pp. 86-101.
4. Al-Naqib, K. M., 1960. Geology of the southern area of Kirkuk Liwa, Iraq. 2nd Arab Petroleum Congress, Beirut, 2, 45-81.
5. AL-Sheikhly S.J.; Tamar-Agha M. and Mahdi M. M., 2015. The facies analysis of the Cenomanian –Turonian succession of Surdash –Shaqlawah area, NE Iraq. *Iraqi Journal of Science* 56(1C):pp.767-773.
6. Archie, G.E., 1942. The Electrical Resistivity Log as an Aid in Determining Some Reservoir Characteristics. *Transactions of the AIME*, 146, 54-62.
7. Asquith, G. and Krygowski, D., 2004. Basic Well Log Analysis. AAPG Methods in Exploration Series, No. 16.
8. Asquith, G.B. and Gibson, C.R., 1982. Basic Well Log Analysis for Geologists. The American Association of Petroleum Geologists (AAPG), Tulsa.
9. Bassiouni, Z., 1994. Theory Measurement and Interpretation of Well Logs.
10. Bates R.L. and Jackson J.A., 1980. *Glossary of Geology*. 2nd Edition, American Geological Institute, Virginia.
11. Bellen R. C., 1956. The Stratigraphy of the 'Main Limestone' of the Kirkuk, Bai Hassan and Qarah Chauq Dag structure in the north Iraq, *Journal Institute of Petroleum*, 42, 393, pp. 233-263.
12. Bellen, R. C. V., Dunnington, H., Wetzel, R., Morton, D. 1959. *Lexique Stratigraphique*, International. Asia, Iraq. 333p.
13. Bowen, D. G., 2003. Formation Evaluation and Petrophysics, 273p.
14. Brock, J. (1986) *Applied Open-Hole Log Analysis*. Volume 2, Gulf Publishing Company, Houston.
15. Buday, T. and Jassim, S. Z., 1987. The Regional Geology of Iraq, Vol.2: Tectonism, Magmatism and Metamorphism. Publication of GEOSURV, Baghdad, 352p.
16. Buday, T., 1980. Regional Geology of Iraq: Vol. 1, Stratigraphy and paleogeography: IIM Kassab and SZ Jassim (Eds). DG of Geological Survey and Mineral Investigation. 445p.
17. Cluff Suzanne G., Cluff Robert M., 2004. Petrophysics of the Lance Sandstone Reservoirs in Jonah Field Sublette County, Wyoming. AAPG Studies in Geology 52 and Rocky Mountain Association of Geologists 2004 Guidebook.
18. Dikkers A. J. 1985. Geology in Petroleum Production. *Developments in Petroleum Science* 20. xiv + 240p.

19. Ditmar, V. and Iraqi-Soviet Team, 1971. Geological conditions and hydrocarbon prospects of the Republic of Iraq (Northern and Central parts). Manuscript report, INOC Library, Baghdad.
20. Doveton, J.H., 1994. Geologic log interpretation. SEPM Short Course No. 29: 169p.
21. Dunnington, H. V, 1958. Generation, accumulation, and dissipation of oil in Northern Iraq. In Weeks, L. G. (ed.) Habitat of Oil, AAPG, Tulsa, Oklahoma, USA, p. 1194-1251.
22. Ellis D.V. and Singer J.M., 2008. Well Logging for Earth Scientists. 2nd Edition, Springer, Berlin.
23. Etnyre, L.M., 1990, Estimation of petrophysical parameters using a robust-Marquardt procedure, paper Q, in 13th European formation evaluation symposium transactions: Society of Professional Well Log Analysts, Budapest Chapter, 20 p.
24. Fouad, S.F. (2012) Tectonic Map of Iraq, Scale 1:1000,000. 3rd Edition, Iraq Geological Survey Publications, Baghdad.
25. Ghafur A.A., 2012. Sedimentology and reservoir characteristics of the Oligocene – Miocene carbonates (Kirkuk Group) of Southern Kurdistan, Ph.D. Thesis, School of Earth and Ocean Sciences Cardiff University, UK.
26. Hamada G. M., 2008. Identification of Hydrocarbon Movability and Type from Resistivity Logs. Petroleum Science and Technology, 26, 6, pp. 638-648.
27. Hilchie D. W., 1978. Applied open hole log interpretation. Colorado, Inc., 309 p.
28. Hingle, A.T., 1959, The use of logs in exploration problems : SEG 29th Annual Meeting.
29. Hook J. R., 2003. An Introduction to Porosity, Petrophysics. 44, 3, pp. 205– 212.
30. Hughes, G. W., Beydoun, Z. R., 1992. The Red Sea-Gulf of Adan: Biostratigraphy, lithostratigraphy and palaeoenvironments. Journal of Petroleum Geology, 15, pp.135-156.
31. Jassim S.Z. and Goff J.C. , 2006. Geology of Iraq. Czechrepublic, Brno, 341 p.
32. Krassay A., 1998. Outcrop and Drill Core Gamma-Ray Logging Integrated with Sequence Stratigraphy: Examples from Proterozoic Sedimentary Successions of Northern Australia. AGSO Journal of Australian Geology and Geophysics, 17, 285-300.
33. Larionov V., 1969. Radiometry of Boreholes. NEDRA, Moscow.
34. Mahdi H.A., Al-Kubaisi M.Sh. and Al-Jawad S.N., 2022a. Microfacies Analysis and Diagenetic Assessment of the Late Oligocene-Early Miocene Succession in Khabaz Oilfield, Northern Iraq. Iraqi Geological Journal, 55 (1D), pp.85-104.
35. Mahdi H.A., Al-Kubaisi M.Sh. and Al-Jawad S.N., 2022b. Structural Study of the Late Oligocene-Early Miocene Sequence in Khabaz Oil Field, NE of Iraq. Iraqi Geological Journal, 55 (1F), pp.70-80.
36. Majid, A. H., Veizer, J. A. N., 1986. Deposition and Chemical Diagenesis of Tertiary carbonates, Kirkuk Oil Field, Iraq. AAPG Bulletin, 70, 898-913.
37. Moradi S., Moeini M., Mohammad Kamal Ghassem al-Askari M. K. G. and Mahvelati E. H., 2016. Determination of Shale Volume and Distribution Patterns and Effective Porosity

- from Well Log Data Based On Cross-Plot Approach for A Shaly Carbonate Gas Reservoir. *Earth and Environmental Science* 44, 042002. pp. 1-7.
38. Pickett, G.R., 1968, A review of current techniques for determination of water saturation from logs : *Jour. Pet. Tech.*, p. 1425-33.
39. Rider M. and Kennedy M., 2011. *The Geological Interpretation of Well Logs*. 3rd Edition. DEWEY: 622.18282. DEWEY edition: 22. Language: English. 432p.
40. Sadooni F.N. and Alsharhan A. S., 2019. Regional stratigraphy, facies distribution, and hydrocarbons potential of the Oligocene strata across the Arabian Plate and Western Iran. *Carbonates and Evaporites*, 34, pp.1757–1770.
41. Schlumberger, 1972. *Log Interpretation Manual/Principles*. Vol. 1. Schlumberger Well Services Inc., Houston.
42. Schlumberger, 1989. *Log Interpretation, Principles and Application*. Schlumberger Wireline and Testing, Houston.
43. Schmoker JW, Krystinich KB, Halley RB., 1985. Selected characteristics of limestone and dolomite reservoirs in the United States. *AAPG Bull* 69,5: pp.733–741.
44. Selley R.C., 1998. *Elements of Petroleum Geology*. Academic Press, London, United Kingdom, 470 p.
45. Shepherd M., 2009. *Rock and Fluid Properties, Oil field production geology: AAPG Memoir*, 91, pp.65-68.
46. Tiab D. and Donaldson E.C., 2004. *Petrophysics: Theory and Practice of Measuring Reservoir Rock and Fluid Transport Properties*, Second Edition. Gulf Professional Publishing is an imprint of Elsevier 200 Wheeler Road, Burlington. 485p.
47. Timur A., 1968. An Investigation of Permeability, Porosity and Residual Water Saturation Relationships for Sandstone Reservoirs. *The Log Analyst*, 9, 3-5.
48. Verma M. K., Ahlbrandt T. S. and Al-Gailani M., 2004. Petroleum reserves and undiscovered resources in the total petroleum systems of Iraq: reserve growth and production implications. *GeoArabia*, Vol. 9, No. 3, 2004. Gulf Petrolink, Bahrain.
- Zhang J. H., Hu Q. and Liu Z. H., 1999. Estimation of true formation resistivity and water saturation with a time-lapse induction logging method, *The Log Analyst*, 40, 2, p.138-148.
-